APPLICATION ADVANCES IN HTS BEARING TECHNOLOGY

Frank N. Werfel, Uta Flögel – Delor, Rolf Rothfeld, Dieter Wippich, Thomas Riedel
Adelwitz Technologiezentrum GmbH (ATZ), Adelwitz, Germany
werfel@t-online.de

ABSTRACT
Superconducting magnetic bearings (SMB) are of increasing technical interest. Based on passive magnetic levitation and the flux pinning effect of melt textured YBCO a number of SMB modules have been developed and tested in prototype machines. The individual bearing components superconductors and permanent magnets and their interaction is investigated. Characterization experiments are conducted to understand the rotor dynamic behavior and the acting forces. In terms of unbalance and critical speeds the suspended wheels and rotors compare favorably with conventional bearing devices. The rationale of our present bearing technology lies in the assembling of a first 30 000 rpm - centrifuge prototype with complete passive HTS bearings. A high-speed 40 mm rotor of a scanning device is accelerated to 174 000 rpm confirming stable low-drag and low energy operation. Finally, the necessary vacuum and cryogenics technology is discussed. Based on experimental results various cooling solutions are suggested.

1. INTRODUCTION

Non-contact bearings, such as electromagnet bearings, overcome problems with friction and mechanical wear and can be made inherently stable with position sensors and electronic feedback control loops. However, the achievement of entirely intrinsic contactless suspension is subject to the fundamental restriction of the Earnshaw theorem. In the practical consequence stability under magnetostatic fields is impossible unless diamagnetic or superconducting materials are used. Due to the improved fabrication of bulk high- temperature superconducting (HTS) material the use of superconducting passive magnetic bearings for high – speed rotational applications is increasingly attractive. HTS components possess a superior physics and technique for electric machines and power application compared to the conventional level. The principal benefit of SMB`s and the main advantages stem from low-drag torque and the self - centering, unlubricated, wear-free and vacuum- compatible operation. The maximum forces and stiffnesses with presently < 1 kN / mm are still smaller compared to active magnetic bearings. However, HTS bearing modules with several kN / mm stiffness are under construction. At high speed operation where the active magnetic bearing loss is proportional to the square of the speed the HTS counterpart has advantages. The price of the self centering: A HTS bearing operates under cryogenic conditions lower than T_c only. We abbreviate this type of passive magnetic bearing therefore simply by “cold bearing”. In contrast to ball bearings, cold bearings are an integrated part of the overall design and cannot be specified in terms of simple mechanical interfaces. Control of the SMB properties such as levitation pressure (load), restoring forces (stiffness) and damping could be of special importance in the applications desired. Hence, and because of the variability new concepts of the complete SMB equipment have to be designed. In the first half decade after the high $-T_c$ discovery many efforts have been made on developing HTS bearing mechanism both from experiments [1-3] and numerical simulation [4]. In contrast to such simple cases, the configuration of magnets and high - T_c superconductors for practical applications such as energy storage flywheels with safety and stability requirements is more complicated. Either the rotors are completely suspended by superconducting thrust bearings in lower position [5,6] or the SMB is combined with active magnetic bearings [7,8] to study stiffness, damping and rotational loss. The efficiency of flywheel devices depend strongly on the coefficient of friction at

higner speeds, which is estimated to be 10^{-3} to 10^{-9} for real loads.

The problem that now exists is besides of demonstrators to develop effective designs of complete HTS bearing devices including vacuum and effective cooling in terms of the parameters weight, speed, power and costs to approach the specific application requirements.

The objective of this paper is to discuss the present status of superconducting passive magnetic bearings to suspend technical wheels and, in particular, to describe the progress in design, development and to present test results on unbalanced rotors and high-speed wheels.

2. HTS BEARING DESIGN

2.1 HTS materials aspects

The key parameter of a superconducting magnetic bearing is the obtained electromagnetic force due to the interaction between a superconductor and a (permanent) magnet. The most prominent and advanced bulk material is melt textured YBCO with a critical current J_c for large samples in the order of 30 - 40 kA/cm² at 77 K and zero applied magnetic field. The maximum trapped field in YBCO is more than 1 Tesla at 77 K, and 14 Tesla at 20 K, presently limited only by the materials tensile strength and degradation. The important material property of the HTS used in cold bearings is the effectiveness of microscopic pinning centres connected with a desired high critical current density $J_{c.}$. High-T_c material is capable to maintain trapped magnetic fields and to produce large attractive and repulsive magnetic forces. Recent results in melt texture fabrication of high quality YBCO bulk superconductors lead to a maximum levitation pressure of 18 N / cm² against a 0.4 Tesla permanent magnet (PM). In general, various materials growing strategies exist in order to provide high performance superconducting bulk material.

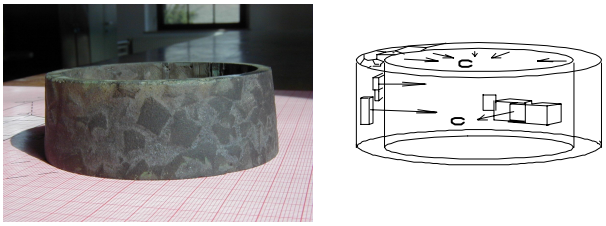

FIGURE 1: YBCO melt textured ring with a preferred grain orientation (right)

Single grain material processed by seeding with MgO or Sm123 is the most prominent and **advanced laboratory fabrication** of YBCO. Recently, several groups have reported the successful growth by seeding a YBCO block approaching 100 mm single domain size [9,10]. The melt texture process requires a stringent control of the extremely slow-cooling growth conditions (0.1-0.3 K/h) and a very long growing time. Even for this large grain material the a-b substructure may not be perfect resulting in a lower intragrain critical current [10]. Hence, the single grain growing strategy will hardly be transferable to an industrial- like HTS fabrication.

FIGURE 2: YBCO plate with 5 and 10 cm single domain structures grown without seeding in 80 hours

For cryomagnetic bearing application we produce **polycrystalline material** with a preferred radial orientation of the sub-domains using a melt texture temperature gradient growth without seeding (**ceramo crystal growth, CCG**) [11]. In Fig. 1 monolithic YBCO ring with a radial-like c axes distribution of the individual Y123 grains is shown. The grain size is about 1 cm. Because of the anisotropic J_c behaviour the alignment of the a-b plane which is the preferred orientation for the supercurrent flow so to have the c-axes parallel to the direction of the external magnetic field increases both the levitation force and stiffness. Our temperature gradient growth is, however, capable to produce large single domain YBCO bulks too. **Without seeding** we fabricated plates **with 5 and 10 cm single domain YBCO** material in a comparable fast 80 hours melt growing process (Fig.2).

Measured levitation forces between polycrystalline cylindrical YBCO bulks and single grain samples give the surprising result that the maximum levitation is less dependent on the grain size as expected, if the critical current J_c is comparable. For practical bearing applications we assume with the polycrystalline monolithic bulks to obtain the adequate HTS material.

Before assembled YBCO rings and cylinders are covered with a metallic copper layer to improve their mechanical and long - life stability. Due to this Cu surface layer on YBCO (and also Bi HTS) the handling and assembling of the HTS components, in particular, the electrical and thermal connections by soldering are substantially easier to perform and more reliable. Their combination with permanent magnets makes it feasible to design SMB modules for rotor loads in the 50 kg level.

2.2 HTS permanent magnet interaction

The bearing forces are strongly dependent on the PM configuration. The design of a magnet bearing is hence of fundamental importance for achieving large electromagnetic forces. Generally, the force exerted by a magnet on a superconductor is given by the gradient of the volume integral

$$F = -grad \int (\boldsymbol{M} * \boldsymbol{B})\, dV \qquad (1)$$

Where $\boldsymbol{M}$ is magnetic moment of the superconductor and $\boldsymbol{B}$ is the field gradient produced by the PM configuration.

A variety of magnet to superconductor configurations is conceivably and their individual performance may differ appreciably. The magnetization of the superconductor $\boldsymbol{M}$ follows a characteristic Bean shape because the interior region is shielded by the induced currents flowing in a thin surface layer of a few millimeter. The penetration depth dx in one dimension is

$$d\boldsymbol{B} / dx = \mu_0 J_c \qquad (2)$$

depending on gradient of the external magnetic flux density $d\boldsymbol{B}/dx$ and the critical current density J_c.

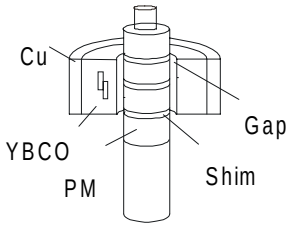

FIGURE 3: Vertical radial HTS bearing structure

From equation (2) it becomes evident that changes of the shape of the superconductor will have almost no effect on the interaction forces. Therefore, the engineering HTS bearing properties in a first approach depend on the magnetic flux density in the gap and the field dependent critical current density J_c of the superconductor.

A typical HTS bearing configuration is shown schematically in Fig. 3 for a radial type bearing. The optimal ring magnet configuration for a given operating gap depend on the ratio of thickness to diameter (aspect ratio), the material and geometry of the shims and the number of the poles.

Generally, in case of large gap (>5 mm) operation a single pole magnet ring gives the highest force density. The magnetic flux distribution is extended to longer distances in the gap. This geometry is recommended for highly unbalanced rotors or long shafts with the tendency to critical (bending) eigenbehavior.

In the small gap region (< 5 mm) the best stiffness parameters are obtained by stapled PM rings on a shaft in opposite polarity (Fig. 4). Due to metallic shims between the rings we achieve,

- a radial magnetic flux distribution from axial magnetized (standard) PM rings
- an improvement of the circular magnetic flux homogeneity
- a magnetic multipole structure with large gradients

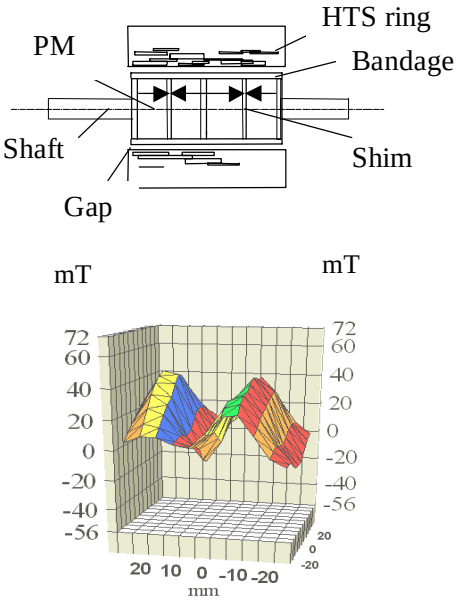

FIGURE 4: Rotor – HTS stator arrangement (top) and measured magnetic flux distribution

Fig. 4 shows a measurement of the flux distribution in the gap for the 4 PM ring arrangement above. With these measurements we optimize the bearing configuration in terms of stiffness and efficient damping.

Besides of the two main components of a HTS bearing, magnet and superconductor, the entire structure of a complete bearing device is more complicated. Usually, a rotor shaft carries two sets of concentric ring magnets to improve the overall stability, in particular, the tilt stiffness. The superconductor on the stator side is assembled by one or more monolithic and polycrystalline cylinders fitting in a Cu housing and connected to a cold stage. Cooling is either achieved by LN_2 in a low cost version or adapted to a cold head of a crycooler (Stirling, GM, Pulse Tube).

To maintain the cryogenics stable during operation either the entire bearing is located in an evacuated tube (< 10^{-2} Pa) or the stator cold side is separated by a thin walled tube of stainless steel or fiberglass. This wall between rotor magnets and the stator HTS surface is a sensitive mechanical element. The wall material have to

be nonmagnetic, mechanical stable and high-vacuum compatible, all conditions at about 1 mm wall thickness! Behind the wall a thermal **super-isolation technology** with **temperature gradients up to 200 K / mm** we have developed and successfully tested. So, a highly compact – sized ∅ 25 mm SMB is consuming as low as 1 L LN_2 per day and hence, causes extremely low operational costs. An integrated cryopumping system serves for the necessary vacuum isolation stable within two months without reconditioning.
Alternatively, various cryocooler systems are operating with bearing demonstrators (3 - 15 W / 80 K Stirling) whereby the bearing temperature can be variable from about 40 K to 80 K.

2.3 Rotor dynamics

An equivalent model for an HTS double - bearing configuration with a top and a bottom bearing is shown in Fig.5. The rotor in the model consists of a rigid body of circular cross section. The equation of motion follows

$$m\ddot{\mathbf{r}} + c\dot{\mathbf{r}} + k\mathbf{r} = F_u \qquad (3)$$

where m is the total mass distribution of the rotor.

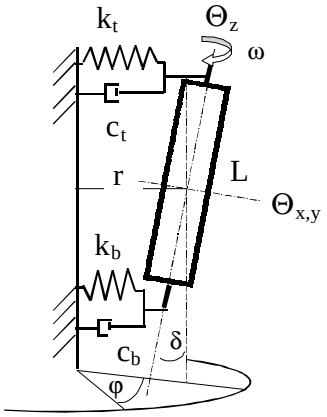

FIGURE 5: HTS bearing model with top and bottom bearing

Each of the two bearings in Fig. 5 are linked to an elasticity and a damping parameter k and c, respectively with an index for the top and the bottom. The vector **r** denotes a set of variables (x, y, z) for the simplified case of parallel displacement. For a tilt motion of the rotor the azimuthal and polar angles φ and δ, respectively are variables, too. Θ is moment of inertia for motions relative to the longitudinal z axis and the transversal x, y axes. L denotes the rotor length.
Assuming constant rotational velocity ω of the rotor the above equation (3) has constant coefficients, and the resulting forces F_u (cos ωt, sin ωt) are harmonical. For a mathematical approach one assumes that the equations contain quantities like displacement and unsymmetry terms that are small of 1st order compared to parameter of the rotor simplifying the calculations.
With the two degrees of freedom in Fig. 5 and the conditions above we are able to calculate the energy, which for the kinetic term is of the form

$$T = \tfrac{1}{2}\,[mr^2\omega^2 + (\Theta_{x,y} - \Theta_z)/\delta^2\omega^2 + \Theta_z\omega^2] \qquad (4)$$

and the potential energy

$$U = \tfrac{1}{2}\,[k_b(r - (L/2)\delta)^2 + k_t(r + (L/2)\delta)^2] \qquad (5)$$

To study the eigenbehavior of the rotor with the expected resonances we obtain the frequency matrix to

$$\begin{vmatrix} (k_b + k_t) - m\omega^2 & L/2\,(k_t - k_b) \\ L/2(k_t - k_b) & (L/2)^2(k_b + k_t) - \Theta\omega^2 \end{vmatrix} = 0 \qquad (6)$$

$$\Theta_{x,y} - \Theta_z = \Theta$$

with the interested angular eigenfrequencies

$$\omega_{1/2} = K/2m\Theta \;+/-\; [K^2/4m^2\Theta^2 - (L^2k_bk_t)/m\Theta)]^{1/2} \qquad (7)$$

$$\text{with } K = [(k_b + k_t)(1/4\,mL^2 + \Theta)]$$

These eigenvalues give the resonances without any damping. However, the damping efficiency of the HTS bearings is one of their key and advantage properties. From equation (3) and Fig.5 the static stiffness values k_b and k_t have to replace by the corresponding dynamic stiffness $k_d(\omega)$

$$k_d(\omega) = dF_u(\omega)/d\mathbf{r} = [(m\omega^2 - k)^2 + \omega^2c^2]^{1/2} \qquad (8)$$

3. TEST RESULTS

3.1 High - speed bearing assembly

Fig. 6 shows a schematic of an operating high - speed double bearing device dedicated for an optical scanning application. Both bearing modules are assembled in a cylindrical double wall copper housing with thermal and vacuum isolation. The shafts with cylindrical 40 and 60 mm rings are machined from one piece so carry two sets of concentric ring magnet configurations. The practical arrangement of PM rings for an optimum flux distribution in the gap were determined by experiments to the field distribution (Fig.4). In a first step we select rotor magnet rings by measuring the circular magnetic flux homogeneity individually, than assembled in pairs in order to obtain for $\Delta B / B_{max}$ less than 1 % whereby $\Delta B = B_{max} - B_{min}$. The PM rings are arranged in opposite polarity with a shim between. How many rings

are sandwiched depend on the gap width and the maximum flux distribution in the gap. Typical flux density values are 0.5 – 1 Tesla.
Cryogenics of the YBCO stator cylinders are in a first

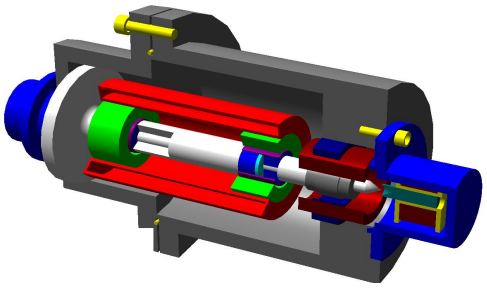

FIGURE 6: Experimental 180 000 rpm optical scanning device using two high-speed HTS bearings

step a cryogenic LN_2 reservoir with respect to the vibrations sensitivity of the device. The drive unit consists of a 3 kHz AC converter accelerating the rotor asynchronously to **about 174 000 rpm**. Alternatively, for extreme stability conditions in the future with a **precision of one rpm at the maximum speed** we have tested and will use an advanced digital drive unit with a hysteresis motor. A moveable mechanics keeps the rotor shaft in a central position relative to the YBCO stator rings during the cool –down procedure.

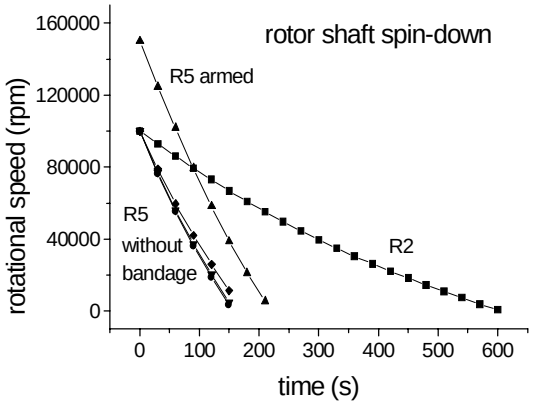

FIGURE 7: Spin-down behaviour of various rotor shafts

With this scanning device in Fig.6 we demonstrate in Fig.7 that the SMB concept does not limit the speed at the level of the bearings. The rationale of the spin-down curves in Fig.7 is the estimation of the energy losses taken from the attenuation of the rotation speed. Large part of the rotor loss is hysteretic in nature and caused by the imperfect magnetization homogeneity of the PM rings. Clearly, the shaft R2 with 2 % homogeneity in the magnetization is less attenuated in speed compared to the rotor with 5 % (R5). The total loss per period $dT_0 / d\omega$ of the shaft R2 in Fig.7 was 38 x 10^{-6} Joule.

With a **rim speed v = 500 m/s** the rotors are designed to accept higher stresses. Most critical and sensitive to the dynamical stress are the NdFeB PM rings which tolerate maximum rim speeds up to 120 m/s only. For higher speeds it is stringent that PM rings are armed. We use either a high quality stainless steel tube or a carbon fibre bandage to protect the magnet rings. Both are fitted to the rings under compression in order to match the radial and tangential dynamical forces to zero at about 70% of the maximum rotor speed. The materials used for a high speed rotors we select very carefully in terms of the specific ultimate tensile strength σ_z / ρ and, in particular, with respect to their long-time stability (e.g. Al alloys tend to degrade in their mechanical properties with time).

3. 2 Unbalance and critical rpm`s

Generally, all rotors are passing so-called critical revolutions due to the effect of unbalance and the resulted gyroscopic forces. In the field of centrifuges and other high - speed machines critical rpm`s are the main source of noise, defects and breakdowns. From engineers standpoint it is therefore desired that for given disturbances in a certain speed range the rotor displacement should have a minimum. In case of the superconducting magnetic bearings the rotor shafts are suspended elastically and move freely in a (air) gap of mm size. Following experimental results, e.g. in Fig. 8a and 8b HTS bearings can accept much higher unbalanced masses compared to conventional bearings. In extreme situations the passive magnetic bearings can handle eccentricity values of a few millimeters and show a stable spin-up into overcritical speed regions. Even in this case of extreme unbalanced rotation the shaft is self-centered and the transmitted vibration to the housing is damped effectively (Fig.8 b).

After passed the phase jump a wheel in a cold bearing is rotating self – centered with the additional benefit of a “balancing effect”. The rotor shaft moves in a certain curve to the position of the mass center. Surprisingly, this curve is not a straight line as one could expect on a first look. Very often an extended semicircel describes the rotor path during the spin – up and spin –down regime.

Useful experiments to study the critical rotor behavior we have performed using a universal measuring and rotor test facility capable to detect the rotor position by a 3 axes position laser detection system. Disturbance pulse and periodical magnetic forces can give to the rotor and measure the response. The test set – up is described in [12]. A typical resonance behavior caused by rotor unbalance is shown in Fig.8.

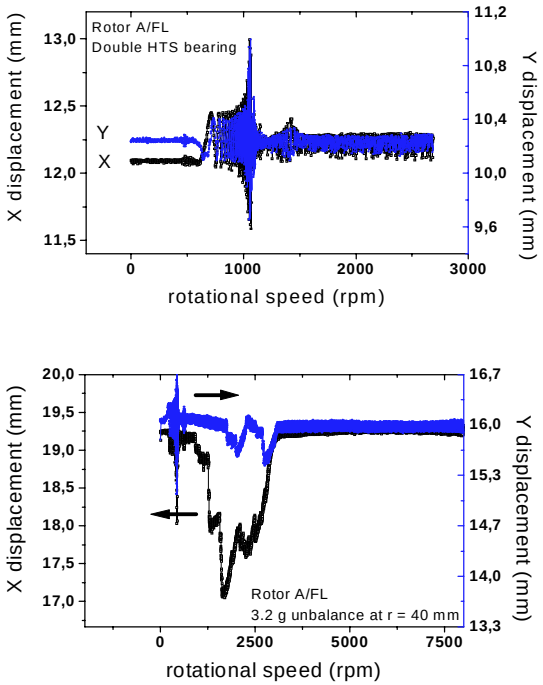

FIGURE 8: Rotor resonance with (bottom) and without unbalance at maximum radius

The 30 cm long rotor was accelerated in a bearing geometry of Fig.5 without balancing. This causes a principal resonance by the rest unbalance at about 18 Hz, followed by a smaller resonance phenomenon at 25 Hz. Up to 600 Hz we do not see further critical frequencies. In the lower part of Fig.8 the rotor behavior under an extreme unbalance indicates resonance amplitudes of more than 2 mm (the gap is 3 mm!). Passing 50 Hz the shaft is stabilized and rotates self-centered and well damped into the high frequency region.

4. CONCLUSIONS

We have investigated superconducting passive magnetic bearings. The experience gained from a model and the experimental approach indicates that passive magnetic suspension is applicable to shafts and wheels up to about 10 kg weights. Engineering prototype high – speed wheel assemblies with passive HTS bearings were fabricated to suspend a centrifugal rotor for 30 000rpm and an optical device rotating presently close to 180 000 rpm at 77 K. Due to air friction the speed of a ∅ 4 cm rotor is limited to about 100 000 rpm. A double – bearing design in vertical geometry with large gap width`s reduces the sensitivity performance to rotor imbalance relative to mechanical bearings by more than a factor of ten. The combination of two bearings of different individual stiffness and damping, respectively improves the dynamical properties in case of periodical or shock vibrations. Measurements of unbalanced wheels by passing critical resonance frequencies give valuable information to bearing properties.

On the basis of HTS materials production we focused our activities in HTS bearing systems technology including the construction of functional prototype power systems and machines with HTS components. The latter one will have a direct response to the materials requirements and to the necessary technology effort. It is concluded that the superconducting magnetic bearings with integrated cooling devices are capable of providing reliable, long – life operation in high-speed rotating machines.

ACKNOWLEDGMENT

The authors would like to thank Dr. G. Zippe and O. Kreißl for valuable suggestions and useful discussions. The practical and straightforward co - operation with ILK Dresden and Heraeus / Kendro, Osterrode is acknowledged. The work was supported in part by the German BMBF under the contract number 13N7247/0.

REFERENCES

[1] Weinberger B. R.; Lynds L. and Hull J. R., Supercond.Sci.Technol.3 (1990) 381
[2] Fukuyama H, Seki K, Takizawa T, Aihara S, Murakami M, Takaichi H and Tanaka S, 1992, Proc 4th Int. Symp. on Supercond.,eds. Hayakawa and Koshizuka, Tokyo Springer- Verlag, 1093
[3] Hull J R, Mulcahy T M, Uherka K L, Erck R A and Abboud R A, Appl.Supercond.vol.2(1994)449
[4] Tsuchimoto M, Homma N, Matsuura K and Matsuda M, Advances in supercond. 9(1997)987
[5] Mulcahy T M, HullJ.R, Uherka K L, Niemann R C, Abboud R G, Juna J.P.Lockwood J A, IEEE Trans. Supercond. 9,2 (1999)297
[6] Kameno H, Miyagawa Y, Takahata R, Ueyama H, IEEE Trans.Supercond. 9,2(1999)972
[7] Coombs T, Campbell A M, Storey R, Weller R, IEEE Trans. Supercond. 9,2(1999)968
[8] Nicolsky R, Gorelov Y, Pereira A.S. David D F B, Santisteban A, Stephan R.M, Ripper A, de Andrade jr R, Gawalek W, Habisreuther T, Strasser T, IEEE Trans. Supercond.9,2(1999)964)
[9] Fujimoto T, Mitsuru M, Masahashi N, Kaneko T, EUCAS`99, Sitges, Spain, preprint
[10] Isfort D, Chaud X, Beaugnon E, Bourgault D, Tournier R, EUCAS`99, Sitges, Spain, preprint
[11] Werfel, F N, Floegel – Delor U, Wippich D, Inst. Phys. Conf. Ser. No. 158 (1997)821
[12] Werfel F N, Floegel – Delor U, Rothfeld R, Wippich D, Riedel T, ICMC`2000, Rio de J. Bras.